

Real-time video signal transmission over a terahertz communication link

Zhen Chen (陈 镇), Li Gu (顾 立), Zhiyong Tan (谭智勇), Chang Wang (王 长),
and Juncheng Cao (曹俊诚)*

Key Laboratory of Terahertz Solid-State Technology, Shanghai Institute of Microsystem and Information Technology, Chinese Academy of Science, Shanghai 200050, China

*Corresponding author: jccao@mail.sim.ac.cn.

Received July 11, 2013; accepted September 4, 2013; posted online November 6, 2013

A 2.4-m communication link operating at 3.9 THz based on a terahertz quantum cascade laser and a terahertz quantum well photodetector (THz QWP) are introduced. The lumped electrical models of THz QWP for small signals are presented. A discussion of the bandwidth limit of the detecting circuit is presented. Using direct on-off-keying modulation and intensity detection, the transmission of digital video signal with a data rate of 2.5 Mb/s is demonstrated. Pseudo-random binary sequences are transmitted to investigate the bit-error rate (BER) at different rates. Result shows the error free transmission when the rate is below 5 Mb/s.

OCIS codes: 200.2605, 140.5965.

doi: 10.3788/COL201311.112001.

Owing to its scientific implications and potential applications in numerous areas, terahertz (THz) technology will soon be at the forefront of development^[1,2]. THz waves are expected to be applied in ultrafast wireless communication, spectroscopy analysis, imaging systems, environmental assessment, and biometric security. In ultrafast wireless communication applications, heterodyne detection, and imaging, the high speed detection of THz waves is indispensable. However, for the detection of THz waves beyond 1 THz, traditional detectors, such as Si bolometers, pyroelectric detectors, and Golay cells which work with measurements of mean power, respond to high-speed signals in an extremely slow manner. THz quantum well photodetectors (QWPs), which hold a potential for rapid response, are promising alternatives.

THz QWP is the very far infrared region extension of the quantum-well infrared photodetectors (QWIP). It is based on intersubband absorption in the quantum well. Owing to its novelty, studies of THz QWPs are minimal; thus, results are limited^[3–6]. Previous investigations have mainly focused on structure design, background-limited infrared performance (BLIP), and many-particle effects. Speed is an advantage of THz QWPs, similar to QWIPs. However, unlike the reported high-frequency capability of QWIPs, research on THz QWP high speed detection has been minimal. In this letter, we report the studies on this subject. We present the lumped electrical models of THz QWP for small signals and discuss the bandwidth limit of the detecting circuit. Likewise, we build a high-speed communication system to investigate the bandwidth limit. To build a communication system with large bandwidth, a fast emitter is necessary. Thus, we adopt THz quantum cascade laser (QCL)^[7]. This study is the attempt to demonstrate digital video signal transmission through a high-speed communication link based on a THz QCL and a THz QWP.

For small signals, the lumped electrical model of the THz QWP is a small capacitor C in parallel with a shunt device-differential resistance R_d and a photocurrent

source I_s (Fig. 1(a))^[8]. Parasitic inductance L is caused by the wire bond. The capacitance is $C = \epsilon_0 \epsilon_r A/h$, where ϵ_0 is the vacuum permittivity, ϵ_r is the relative permittivity of GaAs/AlGaAs, A is the device area, and h is the combined thickness of quantum wells. For the square QWP which we adopt with a side dimension of 1600 μm and a thickness of 3 μm , the C is 98 pF. The shunt resistance R_d can be calculated from the derivation of the voltage-current ($V-I$) curve of THz QWP at the bias voltage. I_s can be derived from the relation $I_s = RP_{\text{in}}$, where P_{in} is the input signal power and R is the responsivity.

When the THz QWP is connected to a cable with an impedance of R_L , and considering the semiconductor physics limiting factor, the power available at frequency ω can be described as $P = \alpha(\omega)\beta(\omega)I_s^2 R_L$. $\alpha(\omega) = 1/[1 + (\omega\tau)^2]$ is due to the photoconductive lifetime, whereas $\beta(\omega) = 8/\left[\left(1 + \frac{R_L}{R_d} - \omega^2 LC\right) + \omega^2\left(R_L C + \frac{L}{R_d}\right)^2\right]$ is the circuit-limited response. For a THz QWP, the photoconductive lifetime is in the order of pico-seconds, resulting in a -3-dB cutoff frequency of several tens of GHz for $\alpha(\omega)$. For $\beta(\omega)$, we obtain $\beta(\omega) = 8/[1 + (\omega R_L C)^2]$ by ignoring the parasitic inductance L and R_L/R_d (for $R_d \geq R_L$), we get). Thus, the $1/2(2\pi R_L C)$ frequency is 32.5 MHz for both $R_L = 50 \Omega$ and $C = 98 \text{ pF}$.

Furthermore, the photoconductive THz QWP has to work under a low bias voltage. We use a voltage feedback amplifier as a trans-impedance amplifier (TIA) to

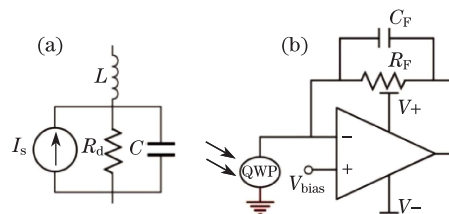


Fig. 1. (a) Electrical model of small signal for the THz QWP; (b) illustration of the TIA circuit.

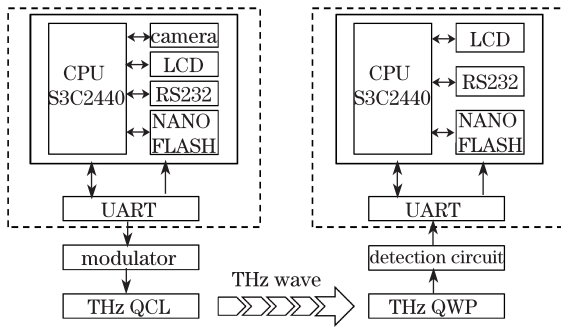


Fig. 2. THz transmission setup.

supply the relatively low bias voltage of 30 mV and to extract the photocurrent to a voltage signal. Figure 1(b) is the illustration of the TIA circuit. R_F is the desired trans-impedance gain. The total capacitance (C_T) on the inverting terminal of the operational amplifier includes the THz QWP capacitance (C_{QWP}) and the parasitic input capacitance (C_{IN}) for the operational amplifier, which has a value of several pF. The practical value of C_{QWP} is 380 pF as measured by an impedance analyzer (4285A, Agilent, USA). The value is derived by adding the capacitance of the cable from the cold section to room temperature to the THz QWP capacitance of 98 pF, which has been previously calculated. To maintain the stability of the circuit, a feedback capacitor (C_F) is placed across R_F . To achieve a maximally flat second-order Butterworth frequency response, the optimum value of C_F is set to $C_F = \sqrt{C_T/[2\pi R_F(GBP)]}$, where GBP is the gain bandwidth product of the operational amplifier. We apply a high gain precision amplifier with low input voltage and current noise, the GBP of which is 1.6 GHz. Theoretically calculated -3 -dB bandwidth of the TIA is $f_{-3dB} = \sqrt{GBP/(2\pi C_T R_F)}$. In the experiment, we found that a value of 10 k Ω for R_F is a good choice. Thus, the calculated C_F is 2 pF and f_{-3dB} is 8.2 MHz. However, if the size of the THz QWP, the capacitance of the cable from the cold section to room temperature, and the trans-impedance R_F are reduced, the -3 -dB bandwidth of the TIA could be in excess of 100 MHz.

We use a THz QCL as the source and a THz QWP as the detector to build a communication link for the transmission of real-time video signal. The scheme shown in Fig. 2 mainly consists of two digital signal ends (dotted line blocks), home-made modulator, detection circuit, THz QCL, and THz QWP.

The THz QCL is based on a four-well resonant-phonon design and a double-metal waveguide. It is attached to a copper heat sink and mounted on the temperature-controlled cold finger of a closed-cycle helium cryostat, and operates at 10 K. The THz QCL is driven by the home-made modulator. The input signal of the modulator, which is supplied by the digital end, is in transistor-transistor logic (TTL) voltage. The voltage controls the high and low switching of the output signal level of the modulator, thereby controlling the output power of the THz QCL. When the output signal of the modulator is high (approximately 13 V, corresponding to a 0.2-A current), the QCL emits THz waves; when the output signal is low (approximately 7.5 V, corresponding to a 0.11-A current), the QCL does not emit waves. Thus,

the on-off-keying modulation is implemented. The high and low levels of the output signal can be adjusted. The maximum modulation speed is expected to be 30 Mb/s.

The emitting 3.9-THz signal from the THz QCL is collected by an off-axis parabolic mirror with a 100-mm focal length and guided along a 2.4-m optical path in room air before it is collected by another off-axis parabolic mirror of the same size and focused onto a THz QWP. The atmospheric absorption for the THz waves is approximately 1.5 dB/m, as measured in the lab environment with 300-K temperature and 47% relative humidity. The THz QWP is a 1600 \times 1600 (μ m) mesa device fabricated from a GaAs/AlGaAs layer structure, which is cooled to 4 K by a continuous-flow liquid-helium cryostat. THz radiation is coupled to the mesa at a 45 $^\circ$ angle. The signal from the photo-conductive THz QWP is processed by the detection circuit. In the detection circuit, the photocurrent of THz QWP is converted by the TIA which is shown in the previous part of this paper, and amplified by a broadband amplifier before it is fed to a low-pass filter with a cutoff frequency of 10 MHz. Subsequently, the signal is sent to a digital signal recovery block. The theoretical bandwidth of the detection circuit is 8.2 MHz as limited by the TIA part, which theoretically allows the passing through of an 8.2-Mb/s pseudorandom binary not-return-zero (NRZ) signal. The output of the detection circuit, which is TTL compatible, is fed back to the corresponding digital end. The process is monitored by an oscilloscope.

Both digital ends comprise ARM CPU, field programmable gate array (FPGA) chip, and other peripheral components. In the digital end of the emitter side, compressed video signals from a camera are channel encoded and sent to the modulator in TTL voltage in the universal asynchronous receiver/transmitter protocol frame by frame. The resolution ratio of the picture frame is 320 \times 240. The bit rate is 2.5 Mb/s. On the receiving side, the digital signals from the detection circuit are sent to the digital end for data decoding, recovering, and displaying.

Figure 3 shows the time traces of signal applied to the emitter (upper trace) and the received signal (lower trace). Despite a delay of about 500 ns, which is mainly caused by the response time of the electrical circuits, the received signal strictly follows the emitting signals. The eye diagram is extinct and open. Figure 4 shows the video transmission results. Due to the superior property of the link, the real-time video signal is perfectly transmitted. The picture recovered in the receiving side is fluent.

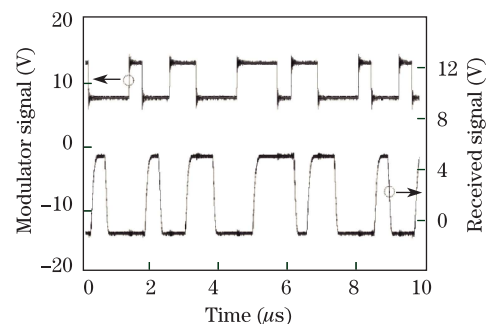


Fig. 3. Time traces of signal applied to emitter (upper trace) and received signal (lower trace).

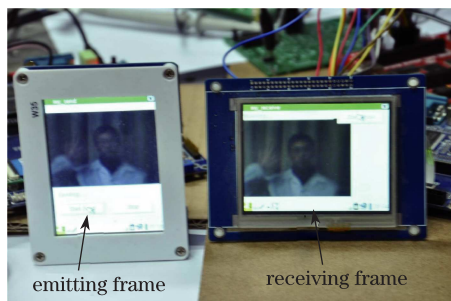


Fig. 4. Video transmission results.

Subsequently, we employ a bit error rate (BER) analyzer to measure the link. The BER analyzer provides an output NRZ signal of pseudo-random binary sequence (PRBS), the bit rate of which can be changed from 1 kb/s to 33 Mb/s. It is used to replace the two digital ends. The output signal of the BER analyzer is introduced at the input of the modulator, and the detection signal is fed back to the BER analyzer. We change the bit rate of the PRBS signal and measure the BER of the link. At a bit rate below 5 Mb/s, the transmission is error free, which shows that the real-time video signal can be transmitted fluently at a rate of 5 Mb/s if the digital ends are improved. BER increases when the bit rate is higher than 5 Mb/s, which can be attributed to the bandwidth limit of the receiving circuit of the THz QWP. As shown by the BER analyzer, desynchronizing occurs when the bit rate exceeds 5 Mb/s and becomes increasingly obvious when the bit rate is higher.

In conclusion, we discuss the lumped electrical models of THz QWP for small signals and the bandwidth limit of detecting circuit. The result shows that the bandwidth is mainly limited by the size of the THz QWP and the capacitance of the cable connecting THz QWP from the cold section to room temperature. We present a THz digital communication link over a distance of 2.4 m, which

employs a THz QCL and a THz QWP. Through this link, the error-free transmission of real-time digital video signal and PRBS signal is implemented. The maximum bit rate is 5 Mbit/s. Our next work focuses on the optimization of the device packaging and the cable link of the device.

This work was supported by the National “863” Program of China (No. 2011AA010205), the National Natural Science Foundation of China (Nos. 61131006, 61176086, and 61204135), the Major National Development Project of Scientific Instrument and Equipment (No. 2011YQ150021), the Important National Science and Technology Specific Projects (No. 2011ZX02707), the Major Project (No. YYYJ-1123-1), and the International Collaboration and Innovation Program on High Mobility Materials Engineering of Chinese Academy of Sciences, and the Shanghai Municipal Commission of Science and Technology (Nos. 10JC1417000, 11ZR1444000, and 11ZR1444200).

References

1. I. Hosako, N. Sekine, M. Patrashin, S. Saito, K. Fukunaga, Y. Kasai, P. Baron, T. Seta, J. Mendrok, S. Ochiai, and H. Yasuda, *Proc. IEEE* **95**, 1611 (2007).
2. T. Nagatsuma, *IEICE Electron. Express* **8**, 1127 (2011).
3. H. Liu, C. Song, A. J. Spring Thorpe, and J. Cao, *Appl. Phys. Lett.* **84**, 4068 (2004).
4. H. Luo, H. Liu, C. Song, and Z. R. Wasilewski, *Appl. Phys. Lett.* **86**, 231103 (2005).
5. X. Guo, Z. Tan, J. Cao, and H. Liu, *Appl. Phys. Lett.* **94**, 201101 (2009).
6. Z. Tan, Z. Chen, J. Cao, and H. Liu, *Chin. Opt. Lett.* **11**, 031403 (2013).
7. S. Kumar, *Chin. Opt. Lett.* **9**, 110003 (2011).
8. P. D. Grant, R. Dudek, M. Buchanan, L. Wolfson, and H. Liu, *Electron. Lett.* **41**, 214 (2005).